Peremennye Zvezdy (*Variable Stars*) **45**, No. 5, 2025

Received 3 January; accepted 17 February.

DOI: 10.24412/2221-0474-2025-45-54-62

Results of Light Curves Analysis for Eclipsing Old Nova V728 Scorpii in Active and Quiet States

I. B. Voloshina[1], T. S. Khruzina[1], A. N. Tarasenkov[1,2]

[1] Sternberg Astronomical Institute, Moscow State University, Universitetskij pr. 13, Moscow 119992, Russia

[2] Institute of Astronomy of Russian Academy of Sciences, 48 Pyatnitskaya Str., Moscow 119017, Russia

The results of light curve analysis are presented for the old Nova V728 Sco. The object is a high-inclination system with an orbital period of $3\overset{\mathrm{h}}{.}32$. The observed light curves of V728 Sco from photometric observations of C. Tappert et al. performed in 2012 were fitted with synthetic light curves to solve for the parameters of this system. We found the system parameters providing the shape of the synthetic light curve most closely matching the observed one applying the Nelder–Mead method. Contributions to the combined flux from the system components: white dwarf, red dwarf, accretion disk with the hot spot on its lateral surface, and hot line are determined for active and quiet states in the frame of the combined model developed by T. S. Khruzina in 2011.

1 History of the variable

The cataclysmic variable V728 Sco (N Sco 1862, also known as N Ara 1862) was discovered on October 4, 1862 by Tebbutt (1878) at the brightness of $\sim 5^{\mathrm{m}}$. Later it was identified with an eclipsing dwarf nova with coordinates $\alpha = 17^{\mathrm{h}}39^{\mathrm{m}}05\overset{\mathrm{s}}{.}58$, $\delta = -45°27'14\overset{''}{.}4$ (J2000; Tappert et al. 2012). The Gaia-DR3 coordinates of this star are very similar: $\alpha = 17^{\mathrm{h}}39^{\mathrm{m}}05\overset{\mathrm{s}}{.}580$, $\delta = -45°27'14\overset{''}{.}39$, equinox and epoch J2000.0. The outbursts in this system occur every $\sim 10-30^{\mathrm{d}}$ with mean duration about 10^{d}. The brightness of V728 Sco during dwarf nova outbursts was $13\overset{\mathrm{m}}{.}5$ and about 15^{m} at quiescence.

Tappert et al. (2013) reported a very interesting behavior of the old Nova V728 Sco and presented some results of their analysis of the star's spectral and photometric observations obtained in the spring of 2012 at the La Silla observatory. It was 150 years after the discovery of the Nova, and the star was very faint, at the brightness level about $17 - 18^{\mathrm{m}}$. The observations were acquired with the ESO NTT telescope in the Bessel V filter as a part of a project to search for post-nova stars and form a sample to compare their properties as a group. Based on the obtained photometric data, light curves were constructed, indicating the presence of a deep eclipse in the system. The orbital period was determined to be $3\overset{\mathrm{h}}{.}32$. At the same time, V728 Sco showed long-term variability, which the authors interpreted as small outbursts like in dwarf novae. This fact and obtained spectroscopic characteristics indicate a relatively low rate of mass transfer in this system. Analysis of low-state eclipse data provides strong, reliable evidence for the existence of a hot inner disk, as predicted by Schreiber et al. (2000) for post-nova stars. From the time of entry to the eclipse and exit from it, the authors estimated the radius of the central object. This value turned out to be larger than the radius of the white dwarf, and the authors interpreted it as the radius of the hot inner region of the accretion disk adjacent to the white dwarf.

Summarizing all the findings, Tappert et al. (2013) conclude that V728 Sco is a very interesting object characterized by unusual history. Therefore they suggested that this object could represent a special class of Novae.

We performed an analysis of photometric observations of V728 Sco obtained on 3 nights, kindly provided to us by Professor N. Vogt and his colleagues. The goal of our work was to determine main parameters of this variable using the method of the light curve solution developed by Khruzina (2011) and earlier used for analysis of photometric observations of different types of cataclysmic variables.

2 Description of the input parameters

The shape of the V728 Sco quiescent light curves is typical of dwarf novae. Such light curves are successfully reproduced within the framework of the standard "combined" model that takes into account the presence of a hot line near the lateral surface of the accretion disk and a hot spot on it on the leeward side of the jet (see Khruzina 2011).

Let us consider the main provisions of the "combined" model. The system consists of a spherical star as a primary component surrounded by an accretion disk, and a red dwarf as a secondary completely filling its Roche lobe. The star is divided into 648 elementary surface areas radiating in accordance with its temperature T_i, depending on the effective temperature of the secondary T_2. When calculating T_i, the heating of the surface of the secondary by radiation from the inner regions of the accretion disk with a temperature of $T_{\rm in}$, $T_{\rm in} \geq T_1$ is taken into account, where T_1 is the effective temperature of the primary. The shape and size of the secondary are set by the parameter $q = M_1/M_2$. When calculating the flow from elementary areas on the secondary's surface, the limb darkening was taken into account in a linear approximation. Gravitational darkening is described by the formula $T_{\rm loc} = T_2(g/g_0)\beta$, where $T_{\rm loc}$ is the local temperature, g is the local acceleration of gravity on the surface of a tidally deformed late-spectral-type star, $\beta = 0.08$ (Lucy 1967). The brightness of an elementary area on the surface of the star is described by the law $dI_\lambda = B_\lambda(T)[1 - u(\lambda, T)(1 - \cos\gamma)]\cos\gamma\ dS$, where γ is the angle between the normal to the elementary area on the surface of the star and the line of sight; $u(\lambda, T)$ is the coefficient of linear darkening to the edge; $B(T)$ is the Planck function; and dS is the area of the considered elementary field. The primary component is modeled by a sphere of radius R_1, which is located in the focus of a weakly elliptical accretion disk with an eccentricity $e \leq 0.2$, a large semi-axis a, and orientation α_e (this is the angular distance in the orbital plane between the periastron of the disk and the line connecting the centers of mass of the components). The disk is optically opaque and has a complex shape: it is geometrically thin near the surface of the white dwarf, and geometrically thick at the outer edge with an opening angle of $\beta_{\rm d}$. The temperature of each elementary area on the disk is determined by the following relation: $T(r) = T_{\rm in}(R_{\rm in}/r)\alpha_g$, where $R_{\rm in}$ is the radius of the first orbit near the primary, $R_{\rm in} \sim R_1$, and the parameter α_g depends on the viscosity of the gas in the disk. In the stationary state of the disk, $\alpha_g = 0.75$; with this value decreasing, the flow from the disk increases significantly due to a more flat distribution of the disk temperature along the radius. When calculating the local temperature of the selected elementary area on the disk, its heating by radiation from the secondary component(this effect is usually insignificant) and heating by high-temperature radiation from the internal areas of the disk are taken into account. Details on other radiating components (Khruzina 2011):

1. The area of collision of the gas flow with the disk, located near its lateral surface. The interaction of the flow and the disk is unstressed, the shock wave occurs in a narrow

area along the edge of the gaseous stream ("hot line"), as a result of interaction of the incoming flows of the disk and the near-disk halo with the jet material. The radiating region of the hot line is represented with a truncated ellipsoid, the center of which is located in the orbital plane inside the disk. The energy release region in the applied model consists of two regions on the surface of a truncated ellipsoid on its windward ($\phi \sim 0.25$) and leeward ($\phi \sim 0.75$) sides outside the disk.

2. A hot spot on the side surface of the disk on the leeward side of the gaseous stream. Here, the radiating region is represented by a half-ellipse, whose center coincides with the point of intersection of the gas-flow axis with the disk. A detailed description of the special code is given in Khruzina (2011).

3 Results of modeling

To solve the inverse problem of determining parameters of the system that has the shape of the synthesized light curve as close as possible to the observed one, the Nelder–Meade method is used (Himmelblau 1972). When searching for the global minimum of the deviation, dozens of different initial approximations were set for each of the light curves, since, the number of independent variables in the studied parameter range being large, there usually is a set of local minima. To assess the consistency of the synthesized and observed light curves, the deviation is calculated according to the formula within the framework of the applied model:

$$\chi^2 = \sum\nolimits_{j=1}^{N} (m_j^{\rm theor} - m_j^{\rm observ})^2 / \sigma_j^2,$$

where $m_j^{\rm theor}$ and $m_j^{\rm observ}$ are magnitudes of the object in the jth orbital phase, obtained theoretically and from observations, respectively, σ is the variance of observations at the jth point, j is the number of a normal point on the average light curve. The values $m_j^{\rm observ}$, σ, and $m_j^{\rm theor}$ are given in Table 1.

Search for optimum model parameters for each light curve was carried out for a grid of q values in the range of $1.3 - 4.5$, with increments $\Delta q = 0.1$; orbital inclination i in the range of $75 - 88^\circ$ with increments $\Delta i = 0.2^\circ$; and R_1/ξ in the range of $0.009 - 0.150$, with increments $\Delta R_1/\xi = 0.0001$, for a wide range of initial values of other system parameters (ξ is the distance between the center of mass of the white dwarf and the inner Lagrangian point L_1, a_0 is the distance between the centers of mass of the stars, $0.5\beta_{\rm d}$ is the half-thickness of the outer edge of the disk in degrees).

Using the obtained parameters, we constructed relations $\chi^2(i)$, $\chi^2(q)$, and $\chi^2(R_1/\xi)$ (see figures below). These figures show the ratio of the current deviation to its minimum value, $\chi^2({\rm rel}) = \chi^2/\chi^2({\rm min})$, for each of the observed light curves for a set of q, I and R.

Table 1: Data for phased light curves of V728 Sco

JD 2456015 ($N = 59$)				JD 2456019 ($N = 37$)				2456063 ($N = 33$)			
ϕ	m(observ)	σ	m(theor)	ϕ	m(observ)	σ	m(theor)	ϕ	m(observ)	σ	m(theor)
0.0055	19.1595	.450E-02	19.17323	0.0033	20.7300	.240E+00	21.04482	0.0069	19.38470	.2335E-01	19.38379
0.0122	19.0850	.301E-01	19.19493	0.0123	20.9250	.130E+00	21.10337	0.0192	19.16700	.6320E-01	19.21192
0.0166	19.0270	.291E-01	19.20703	0.0237	21.0910	.992E-01	20.98532	0.0261	19.04500	.6520E-01	19.01641
0.0210	18.9530	.261E-01	19.14194	0.0396	20.3367	.111E+00	20.44740	0.0325	18.92400	.8540E-01	18.78861
0.0256	18.8640	.251E-01	19.00295	0.0487	19.7060	.751E-01	19.40298	0.0386	18.66000	.4330E-01	18.60223
0.0300	18.7530	.231E-01	18.84699	0.0487	19.7060	.751E-01	19.40298	0.0450	18.56800	.3830E-01	18.34073
0.0344	18.6370	.232E-01	18.66650	0.0532	19.5730	.641E-01	19.33862	0.0512	18.48700	.4940E-01	18.18702
0.0389	18.5050	.192E-01	18.53165	0.0622	19.3397	.127E-01	19.24793	0.0575	18.34100	.4860E-01	18.08025
0.0433	18.4560	.192E-01	18.41560	0.0759	19.2220	.757E-02	19.21528	0.0637	18.18800	.3860E-01	17.97565
0.0477	18.3450	.182E-01	18.20781	0.0895	19.0800	.362E-01	19.20376	0.0699	18.12300	.3150E-01	17.90533
0.0522	18.2620	.162E-01	18.13633	0.1009	18.8425	.505E-01	18.99914	0.0762	18.02600	.2740E-01	17.85583
0.0566	18.2110	.152E-01	18.04809	0.1099	18.7055	.450E-02	18.73841	0.0825	17.95900	.2760E-01	17.80985
0.0610	18.1130	.152E-01	17.96346	0.1235	18.6683	.856E-02	18.69592	0.0887	17.85000	.2450E-01	17.77662
0.0655	18.0550	.142E-01	17.90536	0.1483	18.6516	.888E-02	18.68874	0.0949	17.77000	.2870E-01	17.75000
0.0699	17.9910	.142E-01	17.85118	0.1824	18.6791	.651E-02	18.65911	0.1011	17.68100	.2470E-01	17.72908
0.0743	17.9210	.132E-01	17.81820	0.2141	18.6540	.743E-02	18.63882	0.1137	17.59230	.1262E-01	17.70040
0.0797	17.8700	.132E-01	17.78040	0.2391	18.6396	.424E-02	18.61676	0.1354	17.57800	.9860E-02	17.61980
0.0841	17.8250	.132E-01	17.74932	0.4928	18.4558	.133E-01	18.61292	0.7818	17.31880	.7850E-02	17.32439
0.0908	17.7605	.650E-02	17.72273	0.5157	18.5130	.107E-01	18.61601	0.8210	17.25200	.2031E-01	17.28038
0.0997	17.6980	.340E-01	17.69294	0.6026	18.5004	.749E-02	18.55894	0.8616	17.24670	.1363E-01	17.25328
0.1085	17.6020	.200E-01	17.67528	0.6350	18.5176	.742E-02	18.52507	0.8968	17.26420	.5220E-02	17.27126
0.1174	17.5420	.300E-02	17.61019	0.6840	18.5487	.159E-01	18.42737	0.9130	17.36200	.3550E-01	17.31618
0.1418	17.5052	.643E-02	17.53046	0.7205	18.4281	.202E-01	18.33887	0.9225	17.44800	.1700E-01	17.38146
0.1817	17.4816	.697E-02	17.44590	0.7525	18.3084	.263E-01	18.26824	0.9349	17.53750	.1650E-01	17.49509
0.2183	17.4924	.396E-02	17.43348	0.7843	18.2070	.687E-02	18.21262	0.9442	17.67500	.3190E-01	17.63548
0.2497	17.4594	.126E-01	17.39734	0.8163	18.1659	.130E-01	18.17520	0.9505	17.81000	.4500E-01	17.72922
0.2985	17.4363	.669E-02	17.40241	0.8516	18.1417	.881E-02	18.15906	0.9568	17.96500	.2750E-01	17.95679
0.3500	17.4295	.107E-01	17.33711	0.8848	18.1443	.767E-02	18.17093	0.9631	18.16000	.2940E-01	18.11947
0.3836	17.3511	.719E-02	17.31690	0.9121	18.1566	.709E-02	18.20300	0.9693	18.26400	.3540E-01	18.29915
0.4146	17.3319	.437E-02	17.33547	0.9327	18.2090	.808E-02	18.24765	0.9755	18.46000	.3940E-01	18.42549
0.4457	17.2909	.590E-02	17.33759	0.9465	18.3270	.180E-01	18.32277	0.9819	18.64800	.3420E-01	18.53766
0.4817	17.2867	.214E-02	17.33966	0.9533	18.5850	.302E-01	18.39284	0.9882	18.84700	.5730E-01	18.89410
0.5210	17.2832	.464E-02	17.33874	0.9578	18.8610	.312E-01	18.73218	0.9944	19.11600	.7120E-01	19.06111
0.5483	17.2855	.866E-02	17.33869	0.9624	19.0190	.341E-01	18.85286				
0.5806	17.2912	.318E-02	17.33273	0.9714	19.4030	.379E-01	19.21883				
0.6200	17.2971	.695E-02	17.31517	0.9806	19.5910	.731E-01	19.54504				
0.6496	17.3474	.654E-02	17.32491	0.9852	19.8970	.103E+00	19.67583				
0.6807	17.3752	.505E-02	17.32615	0.9965	20.5160	.160E-01	20.53229				
0.7155	17.3380	.865E-02	17.27641								
0.7457	17.3046	.640E-02	17.26143								
0.7931	17.2501	.622E-02	17.23598								
0.8371	17.1963	.643E-02	17.21017								
0.8615	17.1730	.763E-02	17.20130								
0.8814	17.1990	.801E-02	17.20518								
0.8970	17.2402	.851E-02	17.22025								
0.9132	17.3452	.156E-01	17.26524								
0.9287	17.4607	.561E-02	17.34989								
0.9455	17.7230	.133E-01	17.54469								
0.9500	17.7930	.133E-01	17.59658								
0.9544	17.8780	.143E-01	17.65476								
0.9589	17.9810	.143E-01	17.81286								
0.9633	18.0820	.152E-01	17.94045								
0.9677	18.2010	.172E-01	18.03418								
0.9722	18.2850	.172E-01	18.15612								
0.9788	18.4180	.160E-01	18.32101								
0.9855	18.5560	.202E-01	18.64906								
0.9900	18.7150	.232E-01	18.71060								
0.9944	18.8100	.251E-01	18.76013								
0.9989	19.0450	.291E-01	19.05699								

Figures 1–3 show the ratio of the relative deviation to its minimum value for each of the curves, for different mass ratios q, orbital inclinations i, and radii of the primary component.

Considering the relations we obtained, it is possible to evaluate the basic system parameters:

$$q = M_1/M_2 = 2.5,\ i = 84\overset{\circ}{.}2,\ \text{and}\ R_1 = 0.0154\xi = 0.00913a_0.$$

Effective temperatures we use (averaged over the surface of stars) can change at different times. For example, if there are dark spots on the surface of the secondary, the average temperature will be lower than in the case of their absence. The same situation is with a white dwarf in the case of the presence of a bright accretion zone on its surface. Thus, temperatures of the stars were not fixed and were the desired parameters.

We also searched for main parameters of the other system components (temperatures and sizes of the disk, hot line, and hot spot); they are collected in Table 2.

The observed light curves and those synthesized with the parameters from Table 2 are displayed in Fig. 4.

Figure 5 presents a schematic view of the components of V728 Sco,

Table 2: System parameters from modeling

Parameters	JD 2456015	JD 2456019	JD 2456063
$q = M_1/M_2$	2.5	2.5	2.5
$i, ^\circ$	84.2	84.2	84.2
$\xi,\ a_0$	0.593(3)	0.593(3)	0.593(3)
$R_2,\ a_0$	0.312(3)	0.312(3)	0.312(3)
T_2, K	3140 ± 60	3023 ± 30	2930 ± 50
$R_1,\ \xi$	0.0154(2)	0.0154(2)	0.0154(2)
$R_1,\ a_0$	0.0091(1)	0.0091(1)	0.0091(1)
T_1, K	19500 ± 10	26330 ± 285	22525 ± 150
Disk			
e	0.003(1)	0.023(2)	0.016(5)
$\alpha_e, ^\circ$	113.35(2)	112.2(3)	112.6(6)
$R_\mathrm{d},\ \xi$	0.843(4)	0.598(3)	0.879(2)
$a,\ a_0$	0.498(2)	0.347(3)	0.513(1)
$0.5\beta_\mathrm{d}, ^\circ$	0.60(4)	0.51(1)	0.31(1)
α_g	0.557(1)	0.664(5)	0.477(2)
T_in, K	43035 ± 45	31540 ± 450	33270 ± 225
T_out, K	5495 ± 5	4175 ± 35	5855 ± 30
Hot spot			
R_sp, a_0	0.44(2)	0.29(2)	0.37(2)
Hot line			
$a_\nu,\ a_0$	0.093(1)	0.046(1)	0.048(1)
$b_\nu,\ a_0$	0.297(1)	0.407(1)	0.289(3)
$c_\nu,\ a_0$, was fixed	0.003(1)	0.003(1)	0.003(1)
$\beta_1, ^\circ$	38 ± 5	27.0(1)	48.1(3)
$T_\mathrm{ww,max}$, K	49120 ± 105	26840 ± 750	57630 ± 8050
$T_\mathrm{lw,max}$, K	39435 ± 125	26050 ± 150	45285 ± 510
χ^2	4579 ($N = 59$)	799 ($N = 37$)	404 ($N = 33$)

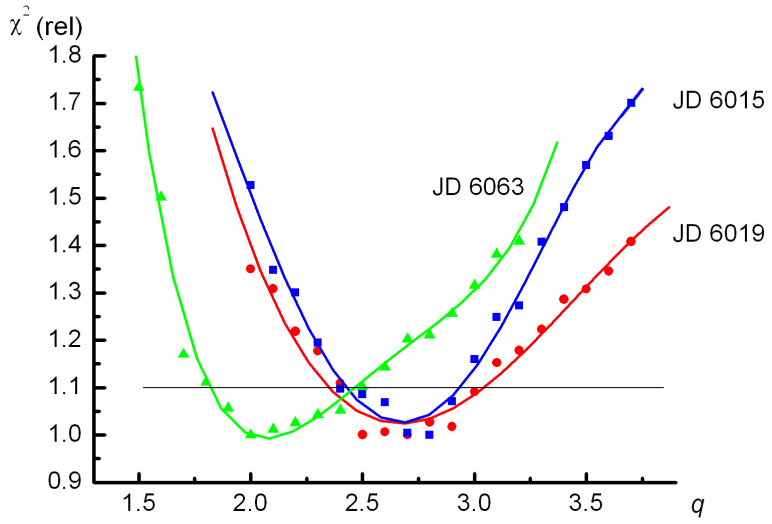

Figure 1.
Relative deviations of q. The value of q acceptable at the χ^2 (rel) level of 1.1 is $q = 2.5$.

Determining the parameters of the V728 Sco system using the Khruzina code not only confirms its usefulness in the case of analyzing photometric data for cataclysmic variables, making this determination more accurate and reliable; the code makes it possible to use the entire light curve for analysis, and not only the eclipse area (as in the case of spectroscopic observations), i.e. it is based on more numerous data. The method was already successfully applied to the analysis of light curves of many dwarf novae and showed good results.

4 Summary

1. We analyzed three observational curves light curves of the cataclysmic variable V728 Sco, believed to be an old Nova, obtained during different stages of its activity[1].

2. We derived the system parameters of V728 Sco. The shape of the synthetic light curve matches the observed one most closely.

3. Contributions to the combined system flux from the different components, such as white dwarf, red dwarf, accretion disk with the hot spot on its lateral surface, and hot line were determined in the frame of combined model (Khruzina 2011) for active and quiet states.

4. The undoubted advantage of the Khruzina code of light curve solution is the use of the entire light curve for determination of system parameters, and not just the area of the eclipse.

Acknowledgements. The study was conducted under the state assignment of Lomonosov Moscow State University.

The authors are very grateful to Dr. C. Tappert, Dr. L. Schmidtobreick, and Prof. N. Vogt for providing photometric observations of V728 Sco.

A. Tarasenkov acknowledges the support of the Foundation for the Development of Theoretical Physics and Mathematics BASIS (project 24-2-1-6-1).

[1]Note by the editor: As of February 17, 2025, the SIMBAD and AAVSO VSX databases give a position for V728 Sco different from that used in the current paper. Nevertheless, the coordinates and the chart in Tappert et al. (2012) agree, and we feel certain that the position published by Tappert et al. corresponds to the star they actually observed. There is less certainty about this star being identical to that discovered by Tebbutt (1878), as claimed by Tappert et al. (2012).

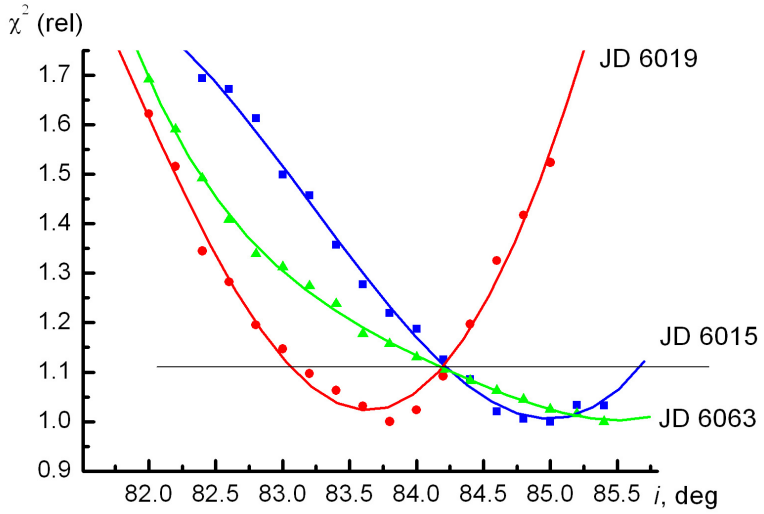

Figure 2.
Relative deviations of i. The value of i acceptable at the χ^2 (rel) level of 1.1 is $i = 84\overset{\circ}{.}2$.

References:

Himmelblau, D. 1972, *Applied nonlinear programming*, Russian translation: 1975, Moscow: Mir Publishers, p. 163

Khruzina, T. S. 1998, *Astron. Rep.*, **49**, No. 10, 783

Khruzina, T. S. 2011, *Astron. Rep.*, **55**, No. 5, 425

Lucy, L. B. 1967, *Zeitschrift für Astrophysik*, **65**, H. 2, 89

Schreiber, M. R., Gänsicke, B. T., & Cannizzo, J. K. 2000, *Astron. & Astrophys.*, **362**, No. 1, 268

Tappert, C., Ederoclite, A., Mennickent, R. E., et al. 2012, *Monthly Notices Roy. Astron. Soc.*, **423**, No. 3, 2476

Tappert, C., Vogt, N., Schmidtobreick, L., et al. 2013, *Monthly Notices Roy. Astron. Soc.*, **431**, No. 1, 92

Tebbutt, J. 1878, *Monthly Notices Roy. Astron. Soc.*, **38**, No. 5, 330

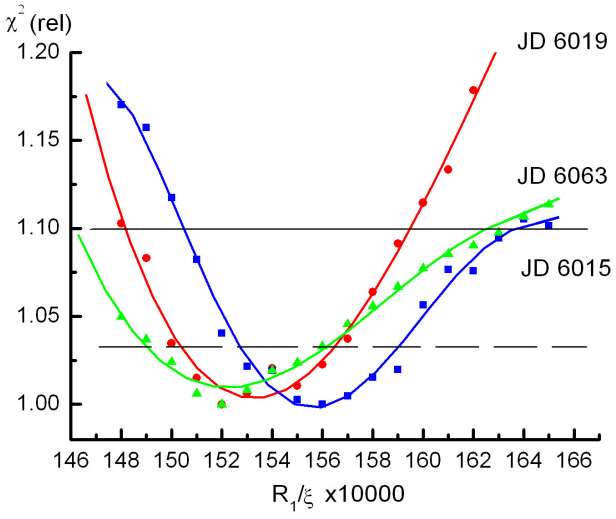

Figure 3.
Relative deviations of R_1/ξ. The value of R_1/ξ acceptable at the χ^2 (rel) level of 1.03 is $R_1/\xi = 0.0154$.

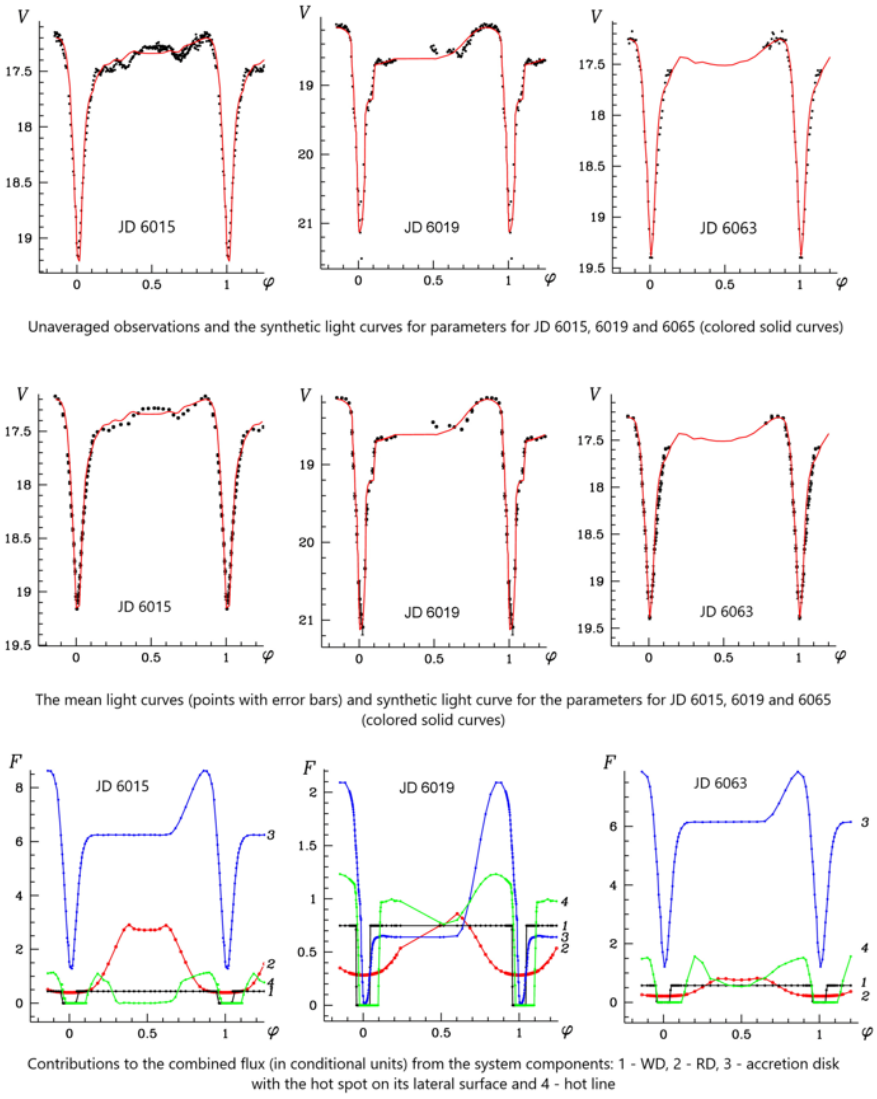

Figure 4.
Folded light curves of V728 Sco and analysis of the contribution of components to them. Truncated Julian dates (with leading figures 245... omitted) are indicated.

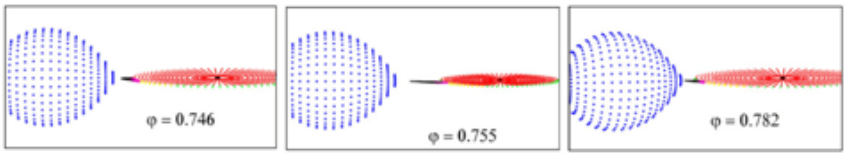

Figure 5.
Schematic views of V728 Sco. Blue: the red dwarf; black: the white dwarf; red: inner disk; green: lateral side of the disk; yellow: hot spot; black: cold part of the hot line; magenta with gradient: heated part of the hot line.